Hindawi
Geofluids
Volume 2022, Article ID 2475021, 19 pages
https://doi.org/10.1155/2022/2475021

Research Article

Mechanical Mechanism Analysis of Roof Fracture Evolution in Stope with Variable Length Based on Elastic-Plastic Structure Theory

Xinfeng Wang,[1] **Mingyuan Lu**,[2] **Rui Wei**,[3] **Zhaofeng Wang**,[4] **and Shan Li**[5]

[1]*College of Environment and Resources, Xiangtan University, Xiangtan, Hunan 411105, China*
[2]*College of Energy and Mining Engineering, China University of Mining and Technology (Beijing), Beijing 100083, China*
[3]*Wangjialing Coal Mine, China Coal Huajin Group Co., Ltd., Hejin, Shanxi 043300, China*
[4]*College of Safety Science and Engineering, Henan Polytechnic University, Jiaozuo, Henan 411105, China*
[5]*College of Qilu Transportation, Shandong University, Jinan, Shandong 250002, China*

Correspondence should be addressed to Xinfeng Wang; wangxinfeng110@126.com

Received 15 November 2021; Accepted 15 March 2022; Published 4 April 2022

Academic Editor: Hualei Zhang

Copyright © 2022 Xinfeng Wang et al. This is an open access article distributed under the Creative Commons Attribution License, which permits unrestricted use, distribution, and reproduction in any medium, provided the original work is properly cited.

Stope with variable length is formed by length change of mining face due to the irregular distribution of geological rock pillars, which is a typical representative of complex coal seam mining. According to the geometric characteristics and mechanical boundaries of each mining stage of stope with variable length, the roof structure models with four boundary conditions were established and solved successively by using the small deflection thin plate bending theory. Combined with the simulated images of MATLAB and FLAC^{3D}, the fracture laws and corresponding engineering phenomena were analyzed. According to the characteristics of roof rock pressure zoning, the overburden structure pressure model of "three stopes, three areas, and three structures" is constructed. The research shows that the traditional "O-X" fracture occurs in the roof of small mining stope. For the cracks generated by prolonged "O-X" fracture and drift "O-X" fracture in mutative mining stope are similar to the crack development characteristics of large mining stope, so they are integrated into full-scale mining stope. The full-scale mining stope roof is broken in "X-O" shape, and the crack continues to develop to produce extended fracture, forming the roof fracture theory of "two stopes and two laws." The research conclusion strongly reveals the failure law of roof from tension instability to plastic fracture and abnormal ground pressure during mining in stope with variable length. It provides a basis for exploring the essence of overburden migration in stope with variable length and strengthening the roof prevention and control theory under the occurrence conditions of deep complex coal seams.

1. Introduction

As the shallow coal seams are gradually exhausted, the deep coal body located in sudden change of coal and rock structures becomes the key object of resource development. However, the mining problems such as complex geological conditions and "three highs and one disturbance" have been strongly affecting the continuity and safety of mining operations [1]. The phenomena of mining pressure are extremely abnormal in stope with variable length, especially when working face is approaching abrupt change of length. The irregular breaking of roof leads to the rapid migration of rock strata. The disturbance impact of hydraulic supports on both sides of working face has obvious spatiotemporal difference. After the sudden change of working face length, resistance of hydraulic supports continues to increase, and when the pressure step distance decreases, roof is broken seriously [2–4]. In addition, due to the influence of soft boundary conditions of the roof in roadway along goaf, coupling relationship between the space-time law of roof

breakage and mining pressure is difficult to be characterized, which leads to great potential safety hazards in mining work, reducing resource recovery and utilization rate.

At present, there are two theoretical bases and corresponding methodologies for the study of roof fracture and overburden migration: beam structure and plate structure. The elastic-plastic deformation in coal body and the variation law of supporting pressure are demonstrated and summarized by analyzing the continuous dynamic fracture of beam structure, when studying disturbance characteristics about coal body caused by hinged fracture of basic roof. This method reflects dynamic migration characteristics and mechanical response mechanism of roof well [5–7]. However, the stope is a three-dimensional working space; beam structure is a one-dimensional model only containing length element, which cannot clearly explain the two-dimensional planar structure characteristics of the roof including width. Therefore, the thin plate theory gradually develops. The overlaying spatial structure engineering theory summarized by Jiang made use of microseismic positioning and monitoring technology that proposed the corresponding fracture forms of roof under different mining environments, thus strengthening the follow-up development of "O-X" fracture [8]. At the same time, in order to explore its specific evolution process in theory, a large number of scholars discussed the rules of roof breakage in stope by establishing a variety of thin plate models with rigid boundaries [9–12], deriving the "O-X" rule of fracture development with different sequences. However, in practical engineering, coal and roof are usually elastic when they are not disturbed and will be transformed into plastic after being disturbed. Therefore, in order to pursue higher precision roof fracture analysis and reveal the whole space-time disturbance characteristics, He, Chen, and Xie used the finite difference principle to build thin plate structure optimization models of elastic foundation boundaries and elastic-plastic foundation boundaries. Based on these, the first excavation of working face in the initial fracture and periodic fracture laws and influencing factors of the basic roof structure were obtained, deepening the roof fracture sequence theories [13–18]. The above theories greatly enrich the theoretical results of "O-X" breaking law under various square boundary conditions. However, when the geological coal and rock distribution are irregular, the roof boundaries of stope will be complicated, that is, the square boundary will change to polygonal boundary, which makes it more difficult to analyze [11]. What is more, the roadway along the goaf is in existence form in deep mining area, due to the influence of mining in adjacent section; the upper roof formed fracture edges. Resulting in the stress distribution of roof boundary and overburden are different from normal [19–24]. Therefore, considering complex boundary conditions, it is difficult to characterize the phenomenon of mining pressure and roof breakage in the stope with variable length, and the theory needs to be improved urgently. It is pressing to reveal the nature of overburden migration in deep stope and strengthen the roof prevention and control mechanism under the complex condition of deep coal seam.

2. Mechanical Model Analysis of Stope Roof with Variable Length

The mining geological characteristics of stope with variable length and the working face from short to long change law of stope are analyzed. Along the strike in turn, it can be divided into small mining, mutative mining, and large mining stope. As shown in Figure 1, coal seam strike per unit length is "a," and coal seam inclination per unit length is "b." The scope of small mining stope is "$2a \times b$," that of mutative mining stope is "$a \times 2b$," and that of large mining stope is "$3a \times 2b$."

Taking the initial mining of short working face as an example, in the deep mining area, in order to decrease the appearance of mining pressure and reduce the difficulty of roadway's maintenance, the roadway close to goaf is reserved as a goaf roadway. The plastic damage degree of the isolation coal pillar in this roadway is very high, resulting in a sharp decline in its clamping capacity for the roof. In addition, roof above the adjacent goaf had already been broken by mining influence of the upper section [18], so all the edges of lower side of the roof in stope with variable length are set as simply supported boundaries. The rest of the roof edges without disturbance and in the stable clamping state are set as fixed boundaries. As the working face advances from small mining stope to mutative mining stope and arrives at large mining stope, the underlying coal mass of the roof decreased, and the roof will be affected by load of the overlying strata and mining disturbance and subject to the corresponding boundary conditions, which lead to continuous fracture.

In view of the above roof boundary characteristics, small deflection thin-plate bending theory of elasticity [25] will be applied to establish the roof elastic model with three sides fixed and one simply supported (the simply supported side is the long side), one side fixed and three sides simply supported, one simply supported with three sides fixed (the simply supported side is the short side), and both sides fixed and both simply supported (the simply supported sides are adjacent). The bending moment numerical value and bending moment image of each stope roof will be obtained by solving the deflection equations using Galerkin method and Ritz method. The breaking laws of roof can be analyzed to reveal the migration nature of roof strata in deep stope with variable length.

2.1. Mechanical Model Analysis of Roof Fracture in Small Mining Stope. Lower boundary of roof in small mining stope has broken in goaf on the upper section, so set as simply supported boundary condition. Due to this stope was the first mining stope, other edges were clamped by strata and coal seam stability, which mechanical conditions were excellent, so set to fixed boundary conditions. Elastic model with three sides fixed and one side simply supported (the simply supported side is the long side) was formed, as shown in Figure 2. By approximate solving the deflection function and bending moment function of this model, the law of fracture evolution of small mining stope can be obtained.

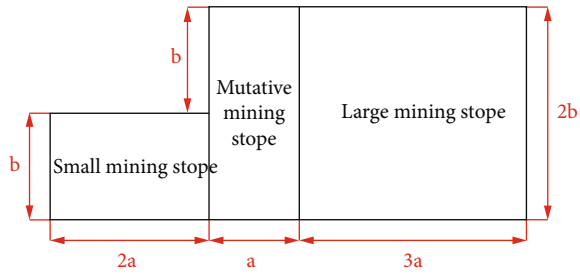

Figure 1: Zoning model of stope with variable length.

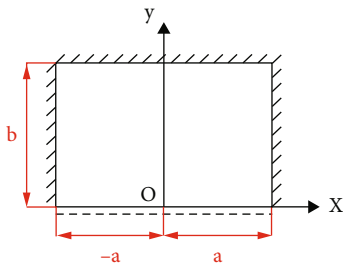

Figure 2: Mechanical model of small mining stope.

According to the condition,

$$\begin{aligned}(w)_{x=\pm a}=0,\left(\frac{\partial w}{\partial x}\right)_{x=\pm a}=0,\\(w)_{y=b}=0,\left(\frac{\partial w}{\partial y}\right)_{y=b}=0,\\(w)_{y=0}=0,\left(\frac{\partial^2 w}{\partial y^2}\right)_{y=0}=0.\end{aligned}\tag{1}$$

In the equation, w is the deflection.

According to Galerkin's method, the deflection equation is

$$w=C_1 y\left(x^2-a^2\right)^2\left(y^2-b^2\right)^2.\tag{2}$$

In the equation, C_1 is constant, and C_2, C_3, and C_4 are the same.

Plug it:

$$\iint_A D\left(\nabla^4 w\right)w_m dxdy=\iint_A q w_m dxdy,$$

$$\Downarrow$$

$$\begin{aligned}\int_0^b\int_{-a}^{a} DC_1[120y\left(x^2-a^2\right)^2+24y\left(y^2-b^2\right)^2\\+2\left(20y^3-12b^2y\right)\left(12x^2-4a^2\right)]y\left(x^2-a^2\right)^2\cdot\left(y^2-b^2\right)^2 dxd\\=\int_0^b\int_{-a}^{a} qy\left(x^2-a^2\right)^2\left(y^2-b^2\right)^2 dxdy.\end{aligned}\tag{3}$$

In the equation, A is the integral interval; D is the bending stiffness of the plate, GPa·m; ∇^4 is the harmonic operator; w_m is the first-order deflection function; q is the load, MPa.

It can be calculated as follows:

$$C_1=\frac{8085q}{2048\left(165a^4b+44a^2b^3+21b^5\right)D}.\tag{4}$$

Then, we can get

$$w=\frac{8085qy\left(x^2-a^2\right)^2\left(y^2-b^2\right)^2}{2048\left(165a^4b+44a^2b^3+21b^5\right)D}.\tag{5}$$

According to the internal force bending moment expression, we can get

$$\begin{aligned}M_x=&\frac{-8085q}{2048\left(165a^4b+44a^2b^3+21b^5\right)}\\&\cdot\left[y\left(12x^2-4a^2\right)\left(y^2-b^2\right)^2+\mu\left(20y^3-12b^2y\right)\left(x^2-a^2\right)^2\right],\\M_y=&\frac{-8085q}{2048\left(165a^4b+44a^2b^3+21b^5\right)}\\&\cdot\left[\mu y\left(12x^2-4a^2\right)\left(y^2-b^2\right)^2+\left(20y^3-12b^2y\right)\left(x^2-a^2\right)^2\right].\end{aligned}\tag{6}$$

In the equation, μ is Poisson's ratio.

Assuming that $A=37.5$ m, $B=50$ m, $q=-15$ MPa, $D=70.52$ GPa · m, and $\mu=0.35$ (the same later) are substituted into the equation. The bending moment expression of this model is calculated by MATLAB to obtain its three-dimensional numerical image, as shown in Figure 3.

Through the analysis of bending moment numerical image, firstly, the bending moments reached its maximum in long fixed boundary midpoint of the plate, causing fixed boundary broke and became a new simply supported boundary. Due to the extreme value of two short fixed boundaries were close to long fixed boundary midpoint maximum, the breakage of short fixed boundaries will be slightly lagging behind long fixed boundary and becoming new simply supported boundaries. Secondly, with the continuous extension of fixed edge fracture, the fracture will be connected with old fracture boundary (the original long simply supported boundary) along the side of goaf roadway, forming an "O-type" fracture circle. Finally, bending moment will take the maximum value the in center of the plate. The fracture will appear in the center of the plate and extend into the "X-type" fracture, namely, the "O-X" fracture law. These are shown in Figure 4.

On the boundary conditions, deep mining stope that use goaf roadway is slightly different from a stope that do not use (three sides fixed and one simply supported/four sides fixed), but "O-X" fracture will occur in all of them. In the process of dynamic roof instability, the accompanying mining pressure phenomena are basically the same. Due to the factors of short length of working face and strike length,

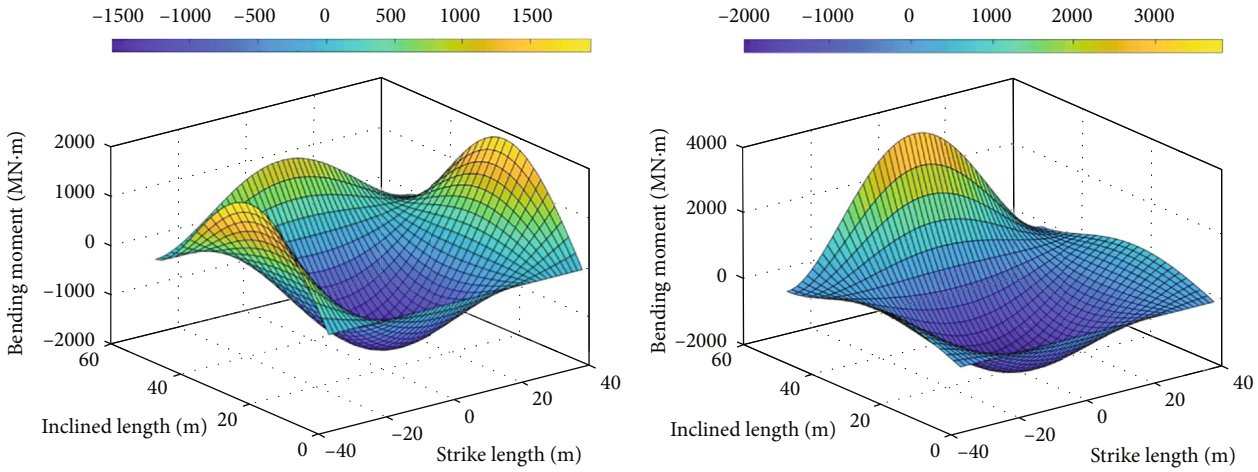

(a) Bending moment M_x

(b) Bending moment M_y

Figure 3: Bending moment of roof model with three sides fixed and one side simply supported (the simply supported side is the long side).

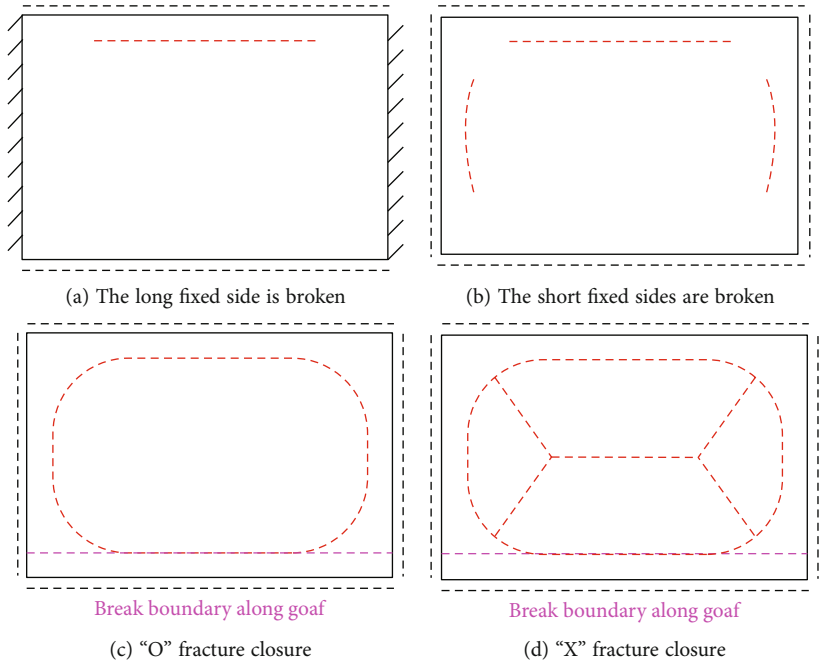

(a) The long fixed side is broken

(b) The short fixed sides are broken

(c) "O" fracture closure

(d) "X" fracture closure

Figure 4: Evolution process of "O-X" fracture in small mining stope.

the dynamic migration of overlying strata will happen moderately, and supporting pressure on the mining space is also small.

2.2. Mechanical Model Analysis of Roof Fracture in Mutative Mining Stope. When mining work of small mining stope was finished, the length of working face will be changing from short to long, entering mutative mining stope. As the working face continues to advance, initial pressure will be generating in mutative mining stope, and roof fracture line above this working face is the right boundary of the stope. In the elastic thin plate bending problems, mutative mining stope boundary for the lower part of 1/2 left side was small mining stope's "O-X" breaking edge, setting it to simply supported boundary, and the left over 1/2 roof was clamped by rock pillars and overlying strata, so set it to fixed boundary. At this point, two kinds of boundary conditions appear on the same edge, which is difficult to effectively calculate and needs to be simplified according to the project situation.

According to the theory of the whole area disturbance characteristic caused by periodic rupture of roof structure, the basic roof fracture will cause the M-shaped or C-shaped rebound compression zone enveloping the working face in front of coal body [15]. Therefore, after completion of mining in small mining stope, a large roof pressure will be generated on basic roof in front of the leading coal wall,

while the adjacent roof of leading coal wall will justly have little influence. Based on the above conditions, the lower half part of mutative mining stope's roof is in the rebound compression region, and considering the weak constraint of boundary conditions, this part can first reach the mechanical limit of fracture [12]. After fracture, stress will redistribute, and then, the second fracture of the upper half of roof will occur in mutative mining stope. This concept of overburden structure fracture with "drift" characteristics reasonably explains the engineering phenomenon of abnormal roof pressure and rapid step-by-step subsidence in narrow area of mutative mining stope.

To sum up, the mutative mining stope was divided into upper and lower parts based on the median line of long side. Just below the dividing line was the goaf, which cannot restrain the rotation deformation of the roof, so set it as simply supported boundary. The breaking order was from I to II. This is shown in Figure 5.

2.2.1. Mechanical Model Analysis of Roof Fracture in Mutative Mining Stope I. This plate's lower edge was the goaf roadway. The left side was broken edge of small mining stope, which was uniformly set as simply supported boundaries, and the right side was sandwich-supported roof between solid coal and overlying rock, which was set as fixed supported boundary, forming an elastic model with one side fixed and three sides simply supported, as shown in Figure 6.

According to the condition,

$$(w)_{x=\pm a/2} = 0, (w)_{y=\pm b/2} = 0, \left(\frac{\partial w}{\partial x}\right)_{x=a/2} = 0. \tag{7}$$

According to Ritz method, let the deflection equation be

$$w = C_2\left(x + \frac{a}{2}\right)\left(x - \frac{a}{2}\right)^2\left(y^2 - \frac{b^2}{4}\right). \tag{8}$$

Plug it:

$$\begin{cases} V_\varepsilon = \dfrac{D}{2}\iint_A \left(\nabla^2 w\right)^2 dxdy, \\ \dfrac{\partial V_\varepsilon}{\partial C_2} = \iint_A q w_m dxdy, \end{cases}$$

$$\Downarrow$$

$$\begin{cases} V_\varepsilon = \dfrac{D}{2}\displaystyle\int_{-b/2}^{b/2}\int_{-a/2}^{a/2}\left[C_2(6x-a)\left(y^2 - \frac{b^2}{4}\right) + 2C_2,\right. \\ \left.\left(x + \dfrac{a}{2}\right)\left(x - \dfrac{a}{2}\right)^2\right]^2 dxdy, \\ \dfrac{\partial V_\varepsilon}{\partial C_2} = \displaystyle\int_{-b/2}^{b/2}\int_{-a/2}^{a/2} q\left(x + \frac{a}{2}\right)\left(x - \frac{a}{2}\right)^2\left(y^2 - \frac{b^2}{4}\right)dxdy. \end{cases} \tag{9}$$

In the equation, V_ε is deformation potential energy.

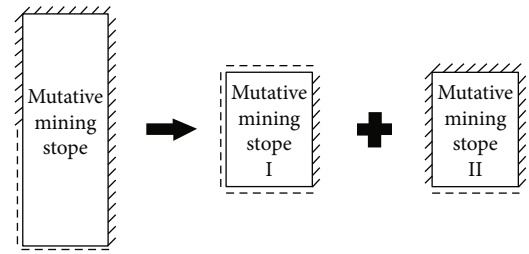

Figure 5: Mechanical model division of mutative mining stope.

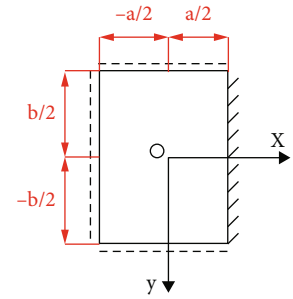

Figure 6: Mechanical model of mutative mining stope I.

It can be calculated as follows:

$$C_2 = \frac{-35ab^2q}{16\left(21b^4 + 6a^4 + 14a^2b^2\right)D}. \tag{10}$$

Then, we can get

$$w = \frac{-35ab^2q(x + (a/2))(x - (a/2))^2\left(y^2 - \left(b^2/4\right)\right)}{16\left(21b^4 + 6a^4 + 14a^2b^2\right)D}. \tag{11}$$

According to the internal force bending moment expression, we can get

$$M_x = \frac{35ab^2q}{16\left(21b^4 + 6a^4 + 14a^2b^2\right)} \cdot \left[(6x-a)\left(y^2 - \frac{b^2}{4}\right) + 2\mu\left(x + \frac{a}{2}\right)\cdot\left(x - \frac{a}{2}\right)^2\right],$$

$$M_y = \frac{35ab^2q}{16\left(21b^4 + 6a^4 + 14a^2b^2\right)} \cdot \left[\mu(6x-a)\left(y^2 - \frac{b^2}{4}\right) + 2\left(x + \frac{a}{2}\right)\left(x - \frac{a}{2}\right)^2\right]. \tag{12}$$

The bending moment expression of this model was calculated by MATLAB to obtain its three-dimensional numerical image, as shown in Figure 7.

In this model, the bending moment M_x obtained the extreme value at the center of long simply supported edge, and bending moment M_y obtained the extreme value at long

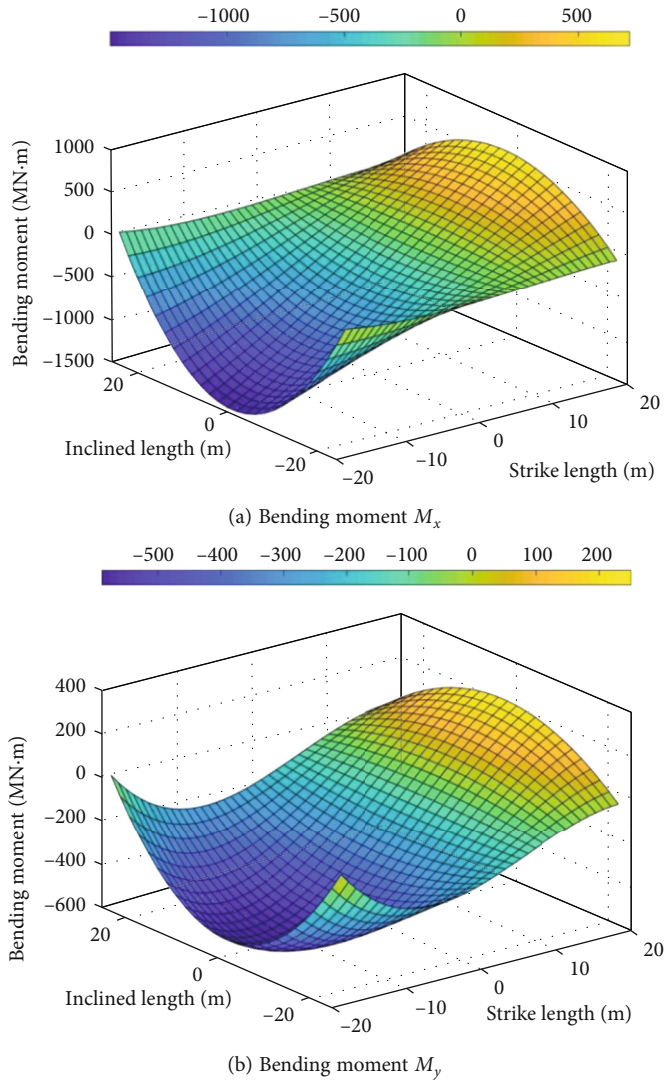

Figure 7: Bending moment of roof model with one side fixed and three sides simply supported.

simply supported edge near the center of plate. It can be concluded that mutative mining stope I broke at center of the long simple supported edge at first, and this boundary coexisted with the fracture boundary of the small mining stope. Then, the fracture will extend along the x-axis to inside of the plate and gradually get closer to fixed supported edge, thus causing instability failure of fixed supported boundary. When the fracture in the center of plate has connected with fixed supported fracture, it will expand to the two short simple supported edges and finally close, forming an "O-X" fracture with extension properties after the small mining stope, as shown in Figures 8 and 9.

2.2.2. Mechanical Model Analysis of Roof Fracture in Mutative Mining Stope II. The roof collapse of mutative mining stope I led to the redistribution of overburden pressure and then caused the roof instability of mutative mining stope II.

Lower boundary in this stope was the broken edge of mutative mining stope I. The middle of two stopes was connected by a hinged structure, so it can be set as simply supported boundary. The rest parts were supported by the stable clamping of rock layer, so they can be set as fixed supported boundaries, forming an elastic model with three sides fixed and one side simply supported (the simply supported side is the short side), as shown in Figure 10.

According to the condition,

$$\begin{aligned}(w)_{x=\pm\frac{a}{2}} &= 0, \left(\frac{\partial w}{\partial x}\right)_{x=\pm\frac{a}{2}} = 0,\\ (w)_{y=b} &= 0, \left(\frac{\partial w}{\partial y}\right)_{y=b} = 0,\\ (w)_{y=0} &= 0, \left(\frac{\partial^2 w}{\partial y^2}\right)_{y=0} = 0.\end{aligned} \tag{13}$$

According to Galerkin's method, let the deflection equation be

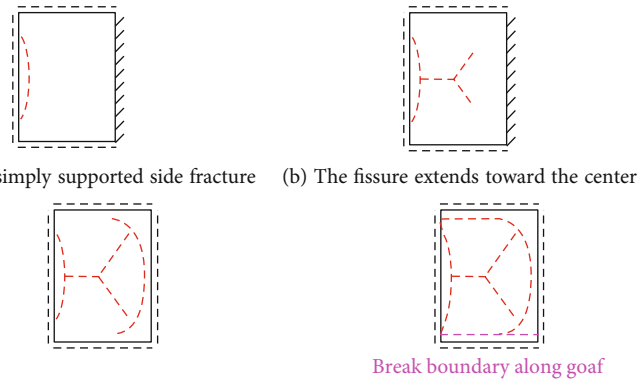

(a) The long simply supported side fracture (b) The fissure extends toward the center

(c) The fixed side breaks and closes (d) The two simply supported sides are through

Figure 8: Fracture evolution process of mutative mining stope I.

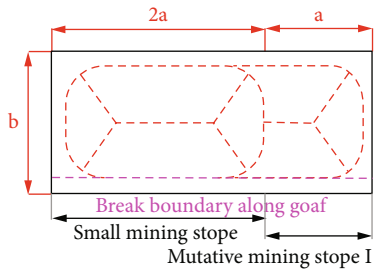

Figure 9: Prolonged "O-X" fracture of subsequent small mining stope.

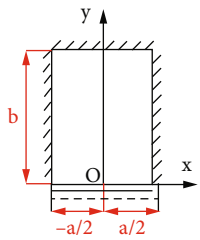

Figure 10: Mechanical model of mutative mining stope II.

$$w = C_3 y\left(x^2 - \frac{a^2}{4}\right)^2 \left(y^2 - b^2\right)^2. \tag{14}$$

Plug it:

$$\iint_A D\left(\nabla^4 w\right) w_m dxdy = \iint_A q w_m dxdy,$$

$$\Downarrow$$

$$\int_0^b \int_{-a/2}^{a/2} DC_3 \left[120y\left(x^2 - \frac{a^2}{4}\right)^2 + 24y\left(y^2 - b^2\right)^2 + 2\left(20y^3 - 12b^2 y\right)\left(12x^2 - a^2\right)\right] y\left(x^2 - \frac{a^2}{4}\right)^2 \cdot \left(y^2 - b^2\right)^2 dxdy$$

$$= \int_0^b \int_{-a/2}^{a/2} qy\left(x^2 - \frac{a^2}{4}\right)^2 \left(y^2 - b^2\right)^2 dxdy. \tag{15}$$

It can be calculated as follows:

$$C_3 = \frac{8085q}{128\left(336b^5 + 176a^2b^3 + 165a^4 b\right)D}. \tag{16}$$

Then, we can get

$$w = \frac{8085qy\left(x^2 - a^2/4\right)^2 \left(y^2 - b^2\right)^2}{128\left(336b^5 + 176a^2b^3 + 165a^4 b\right)D}. \tag{17}$$

According to the internal force bending moment expression, we can get

$$M_x = \frac{-8085q}{128\left(336b^5 + 176a^2b^3 + 165a^4 b\right)} \cdot \left[y\left(12x^2 - a^2\right)\left(y^2 - b^2\right)^2 + \mu\left(20y^3 - 12b^2 y\right)\left(x^2 - \frac{a^2}{4}\right)^2\right],$$

$$M_y = \frac{-8085q}{128\left(336b^5 + 176a^2b^3 + 165a^4 b\right)} \cdot \left[\mu y\left(12x^2 - a^2\right)\left(y^2 - b^2\right)^2 + \left(20y^3 - 12b^2 y\right)\left(x^2 - \frac{a^2}{4}\right)^2\right]. \tag{18}$$

The bending moment expression of this model was calculated by MATLAB to obtain its three-dimensional numerical image, as shown in Figure 11.

This model is compared with the small mining stope roof model with three sides fixed and one simply supported side (the simply supported side is the long side), and the inner part of plate bending moment greatly reduced and has a small cut with bending moment of fixed sides. But in general, bending moments of the maximum point still appear in long fixed side, and simply supported side has slight offset, which induce the initial rupture.

When the two long fixed sides of mutative mining stope II produced cracks, the constraint on bending moment transmission was reduced sharply. The fixed support will

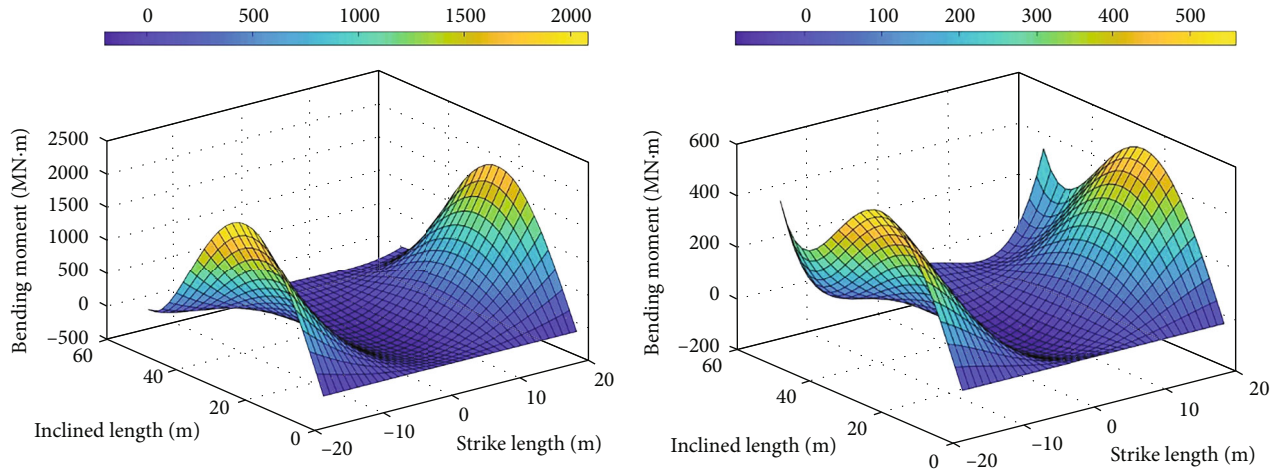

(a) Bending moment M_x

(b) Bending moment M_y

FIGURE 11: Bending moment of roof model with three sides fixed and one side simply supported (the simply supported side is the short side).

transform into simple support condition, and plate with three sides fixed and one side simply supported (the simple supported side is the short side) will transform into the plate with three sides simply supported and one side fixed, which is similar to mutative mining stope I, and then, the corresponding regularity of fracture can be generated. In other words, the crack in the center of initial simply supported edge will start to extend to the center of the plate and gradually get close to the short fixed supported edge to trigger fracture. Finally, it will close with simply supported edge on both sides to complete the secondary fracture of mutative mining stope, as shown in Figure 12.

In terms of the direction of open-off cut in small mining stope, the "O-X" fracture extending along the strike has drifted to inclined direction, as shown in Figure 13. This fracture law is consistent with the roof subsidence rule in the section of mutative mining stope in practical engineering. The law of prolongated "O-X" fracture and drifting "O-X" fracture produced in mutative mining stope is very complex. The entropy value of cutting roof control system is high, which is consistent with the phenomena in support engineering, such as short pressure step distance, high variable pressure strength, and difficult support of broken roof. As a whole, the temporal and spatial relationship between mining advancement and rock migration shows the drift of roof structure fracture, the continuity of rock structure instability, the migration of support pressure expansion, and the instantaneous increase of mining pressure phenomena.

2.3. Mechanical Model Analysis of Roof Fracture in Large Mining Stope. After the roof of mutative mining stope has broken twice, the phenomena of variable pressure and abnormal movement tend to be stable. It means that stope face enters large mining stope. Compared with small mining stope, the support space in the large mining stope is obviously expanded. It still has a trend of continuously increasing support pressure due to restriction of rock structure adjustment and the influence of residual energy release from mutative mining stope.

In engineering practice, when the length of working face reaches 100 m, the roof caving step is generally about 30 m [26]. According to calculated data simulated by MATLAB above, the inclined and strike lengths of roof model in large mining stope both exceed 100 m. In other words, when there is advanced unit distance on the$x$-axis, there will occur once basic roof period break, and there will be three times in total. However, after each break, boundary conditions and plate parameters will not change, and the breaking structure will not change either. Therefore, only the model range of "$a \times 2b$" was taken as the calculation boundary of single roof fracture. The left side and the lower side of model were the fracture roof edges of goaf, which can be set as simply supported boundary condition. The right side and the upper sides were the roof edge of coal layer clamped, which can be set as fixed boundary condition, forming an elastic model of two sides fixed and two sides simply supported (the simple support edges are adjacent), as shown in Figure 14.

According to the condition,

$$\begin{aligned} (w)_{x=0} &= 0, \left(\frac{\partial^2 w}{\partial x^2}\right)_{x=0} = 0, \\ (w)_{x=a} &= 0, \left(\frac{\partial w}{\partial x}\right)_{x=a} = 0, \\ (w)_{y=0} &= 0, \left(\frac{\partial^2 w}{\partial y^2}\right)_{y=0} = 0, \\ (w)_{y=2b} &= 0, \left(\frac{\partial w}{\partial y}\right)_{y=2b} = 0. \end{aligned} \tag{19}$$

According to Galerkin's method, let the deflection equation be

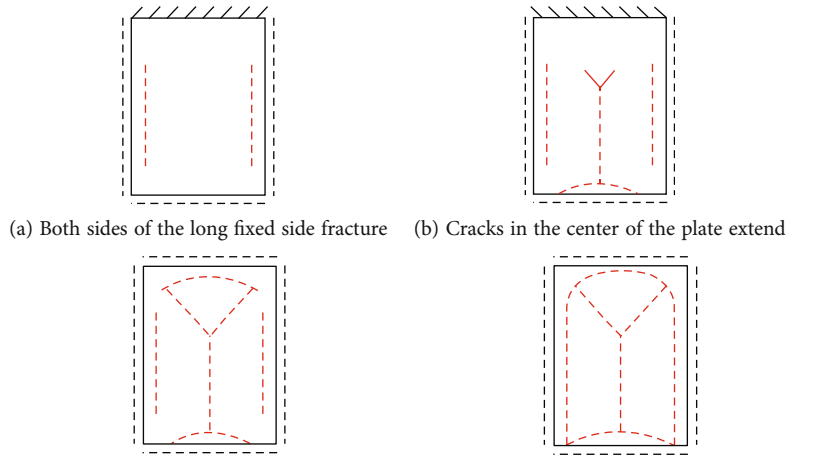

(a) Both sides of the long fixed side fracture (b) Cracks in the center of the plate extend

(c) The short fixed side breaks and closes (d) The two simply supported sides are through

Figure 12: Fracture evolution process of mutative mining stope II.

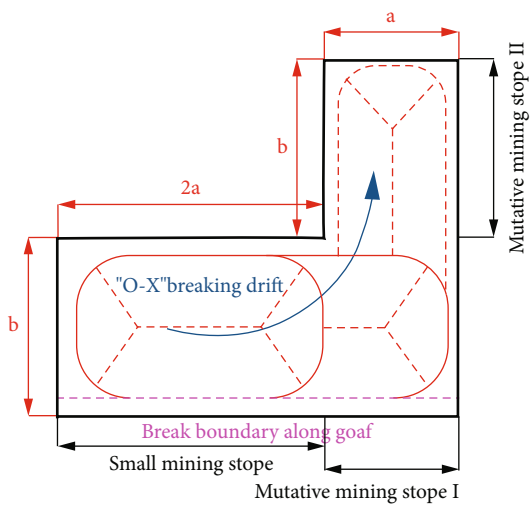

Figure 13: Drift-shaped "O-X" fracture of subsequent small mining stope.

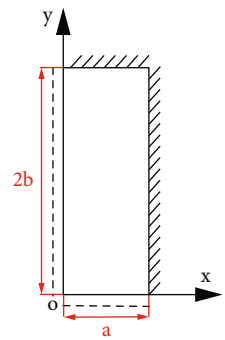

Figure 14: Mechanical model of large mining stope.

$$w = C_4 xy\left(x^2 - a^2\right)^2\left(y^2 - 4b^2\right)^2. \tag{20}$$

Plug it:

$$\iint_A D\left(\nabla^4 w\right) w_m dxdy = \iint_A q w_m dxdy,$$

$$\Downarrow$$

$$\int_0^{2b}\int_0^a DC_4\left[120yx\left(x^2 - a^2\right)^2 + 120xy\cdot\left(y^2 - 4b^2\right)^2 + 2\left(20y^3 - 48b^2y\right)20x^3 - 12a^2x\right]xy\left(x^2 - a^2\right)^2\left(y^2 - 4b^2\right)^2 dxdy$$

$$= \int_0^{2b}\int_0^a qxy\left(x^2 - a^2\right)^2\left(y^2 - 4b^2\right)^2 dxdy. \tag{21}$$

It can be calculated as follows:

$$C_4 = \frac{121275q}{65536\left(45a^5b + 176a^3b^3 + 720ab^5\right)D}. \tag{22}$$

Then, we can get

$$w = \frac{121275qxy\left(x^2 - a^2\right)^2\left(y^2 - 4b^2\right)^2}{65536\left(45a^5b + 176a^3b^3 + 720ab^5\right)D}. \tag{23}$$

According to the internal force bending moment expression, we can get

$$M_x = \frac{-121275q}{65536\left(45a^5b + 176a^3b^3 + 720ab^5\right)} \cdot \left[y\left(20x^3 - 12a^2x\right)\left(y^2 - 4b^2\right)^2 + \mu x\cdot\left(20y^3 - 48b^2y\right)\left(x^2 - a^2\right)^2\right],$$

$$M_x = \frac{-121275q}{65536\left(45a^5b + 176a^3b^3 + 720ab^5\right)} \cdot \left[\mu y\left(20x^3 - 12a^2x\right)\left(y^2 - 4b^2\right)^2 + x\cdot\left(20y^3 - 48b^2y\right)\left(x^2 - a^2\right)^2\right]. \tag{24}$$

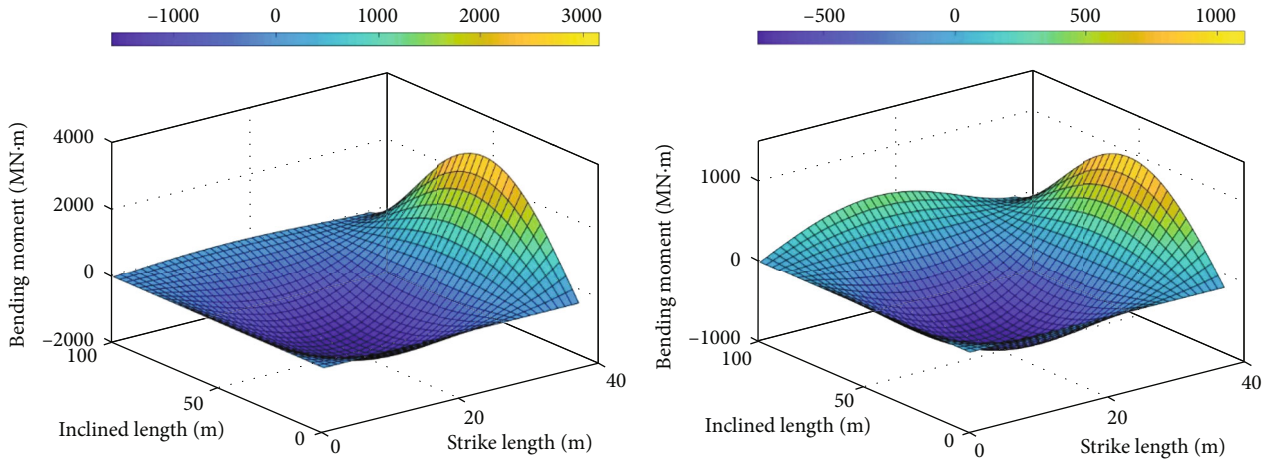

(a) Bending moment M_x (b) Bending moment M_y

FIGURE 15: Bending moment of roof model with two sides fixed and two sides simply supported (simply supported sides are adjacent).

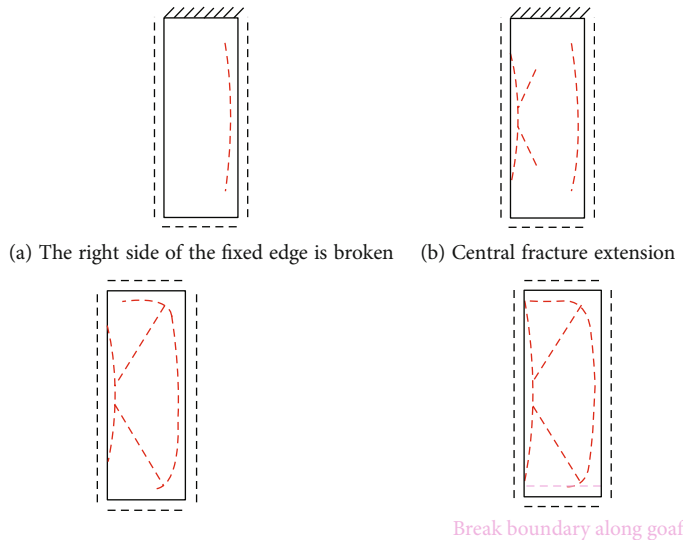

(a) The right side of the fixed edge is broken (b) Central fracture extension

(c) The upper side of the fixed edge fracture and through (d) Simply supported side through

FIGURE 16: Fracture evolution process of large mining stope.

The bending moment expression of this model was calculated by MATLAB to obtain its three-dimensional numerical image, as shown in Figure 15.

At the right side of large mining stope, the maximum bending moment was obtained on fixed edge. The roof model with both sides fixed and both sides simply supported (the simply supported sides are adjacent) will transform into a model with three sides simply supported and one side fixed, similar to the mutative mining stope I. Then, fracture will take place inside the plate close to long side of the simply supported. For the plate is relatively long and narrow, under the action of the corner effect, central crack will extend diagonally to the two corners and intersect with the right side of fixed edge cracks, which will promote upper fixed edge fracture and finally form closure, as shown in Figure 16.

Subsequent sections of large mining stope will form the same type of joint fracture. The stoping advance speed and support quality of this stope can be effectively controlled, and boundary conditions are continuous, so the fracture is regular. However, the length of working face is long, the roof control range is large, and the roof is broken regularly in a wide range, so the periodic pressure step distance is short, and space-time disturbance range caused by it is great. As a result, it has the characteristics of high dynamic pressure higher than the static pressure and will increase in a short time.

After calculation of four kinds of elastic bending thin plate theoretical models and the related numerical analysis, the roof broken whole structure of stope with variable length was finally formed, as shown in Figure 17, which is "small mining stope + mutative mining stope (I and II) + large mining stope."

2.4. Analysis of Integrated Model for Roof Fracture in Mutative Mining Stope and Large Mining Stope. In the

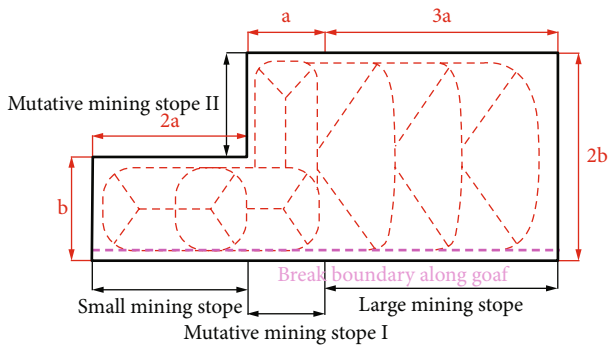

Figure 17: Overall broken structure of stope roof with variable length.

fracture analysis of mechanical model mentioned above, the stope with a working face length of 2*b* was divided into the mutative mining stope (I and II) and the large mining stope. This model can reasonably explain the complex roof disturbance breaking law, but dynamic evolution process is complicated. In the engineering field, after completion of mining in small mining stope, the working face advancement is still continuous and gradual. Although mutative mining stope has the most serious mining pressure, the most intensive roof movement, and the most difficult stope partition that is difficult to solve and deal with, the proportion of recoverable reserves and duration of mining and support work is the least. Considering factors such as working hours and efficiency and practical application of theory, it should be properly integrated with the larger mining stope with a larger proportion of stoping duration.

The theoretical model can be simplified by integrating the different fracture laws of mutative mining stope and large mining stope, which is beneficial to grasp the overall view of stope roof control theory. In following sections, mutative mining stope and large mining stope are collectively referred to as full-scale mining stope, as shown in Figure 18.

This model is an integrated stope by the strike length as the main guide. Through the overview analysis of fracture, the whole fracture law of full-scale mining stope can be obtained. At the lower part of left boundary of full-scale mining stope, there was an initial fracture generated by "O-X" fracture edge of small mining stope, which developed along the strike to inside of full-scale mining stope, and then, the upper part of left boundary fracture occurred and extended along the dip to inside of full-scale mining stope; finally, the two extended fractures converged. This was general law of mutative mining stope (I and II), in which the jumble fracture details were ignored and the "half-X-shaped" fracture was formed. The fracture of mutative mining stope I was the hypotenuse of lower part of the "half-X," while the fracture of mutative mining stope II was the hypotenuse of upper part of the "half-X," as shown in Figure 19.

Initial fracture occurred in long fixed side of the large mining stope, then cracks in the center of plate extended to the two sides and closed with long fixed side, and the two closed to short fixed side, finally causing it to break.

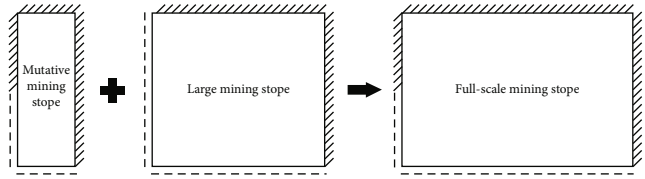

Figure 18: Full-scale mining stope model.

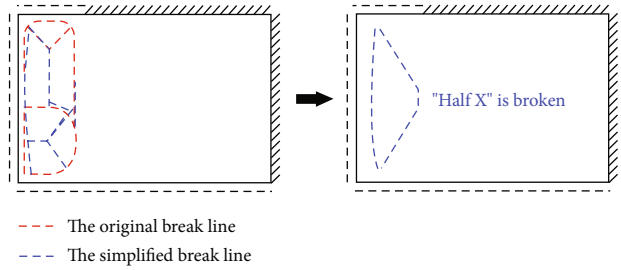

Figure 19: "Half X-shaped" fracture in full-scale mining stope.

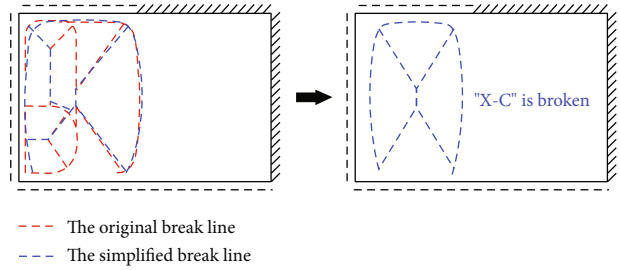

Figure 20: "X-C-shaped" fracture in full-scale mining stope.

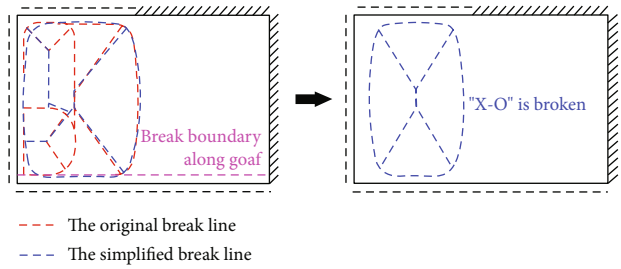

Figure 21: "X-O-shaped" fracture law in full-scale mining stope.

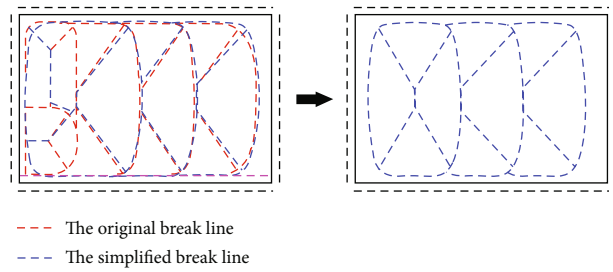

Figure 22: Fracture law of prolonged "X-O" fracture.

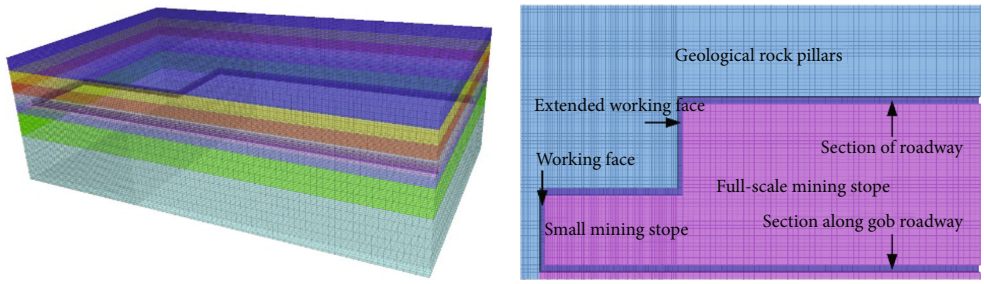

(a) Modeling figure (b) Top view of stope

Figure 23: FLAC^{3D} modeling schematic.

From the perspective of full-scale mining stope, fracture in the center of plate was further broken and expanded from "half X" to "full X" shape fracture, and all fixed sides became "∩" shape fracture, which can be called "C" shape for convenient description. To sum up, the second large-scale fracture of full-scale mining stope was "X-C" shape, as shown in Figure 20.

The "X-C-shaped" fracture was connected with the edge of goaf in the upper section at the lower part of full-scale mining stope, forming a "C-shaped" to "O-shaped" closure, as shown in Figure 21. The final occurrence of the roof in full-scale mining stope is similar to "O-X" fracture, but the development law of "X-O" fracture is slightly different, namely, from the traditional ① long fixed supported sides fracture ⟶ ② short fixed supported side fracture ⟶ ③ the "O" shape closed ⟶ ④ center fracture ⟶ ⑤ "X" shape closed ⟶ ⑥ "O-X" breakage form (form the "O" shape before forming an "X"). It is transformed into ① simple and fixed edge fracture ⟶ ② "half-X-shaped" fracture ⟶ ③ extension of long fixed edge and plate center fracture to induce short fixed side fracture ⟶ ④ "X-C-shaped" fracture ⟶ ⑤ "O-shaped" closure ⟶ ⑥ "X-O-shaped" fracture formation (first form "X" shape and then forming "O" shape).

As the working face continues to advance, the roof caving will occur periodically, and the fracture law is the same as the continuous fracture of large mining stope. The prolongated "X-O" fracture is formed with the roof in mutative mining stope, as shown in Figure 22.

3. Mechanical Characteristic Analysis of Roof Fracture Evolution in Stope with Variable Length

3.1. Establishment of Numerical Model. In order to verify the accuracy of mathematical model, explore the dynamic law of roof instability in stope with variable length, and consider universality of fracture theory in practical engineering problems. The following will use FLAC^{3D} software to establish corresponding coal seam and mining model, through the analysis of coal seam in multistage mining process of plastic zone development and change rules, to provide a strong support for fracture theory in this paper.

The cuboid model of 250 m × 150 m × 80 m was established, and Molar Coulomb model was adopted, fixing boundaries on the four sides and the bottom. An in situ stress of 15 MPa downward along the z-axis was applied on the top of model. The thickness of floor was 50 m, the thickness of coal seam was 3 m, and the thickness of roof was 27 m. The width of working face was 3 m, and the width of section roadway was 4 m. When section roadway was excavated in coal seam, strike length of small mining stope was 75 m and inclined length was 50 m. In this area, three stoping stages were simulated and grid was encrypted. The strike length of full-scale mining stope was 150 m, and the inclined length was 100 m. In this area, four stoping stages were calculated by simulation. The first stoping stage of full-scale mining stope was mutative mining stope zoning, and the last three stoping stages were large mining stope zoning, as shown in Figure 23.

3.2. Analysis of Mechanical Characteristics of Roof Fracture in Small Mining Stope. The small mining stope was divided into three mining calculations, and the roof plastic zone failure analysis was carried out once for every 25 m advancing average. The distribution characteristics of roof stress zone and plastic zone along with work progress are shown in Figures 24 and 25.

The lower part of roof boundary of small mining stope was the broken roof along the goaf. When the initial excavation of small mining stope advanced for 25 m, the stress concentration occurred in the lower part of the left and right sides of goaf. However, due to the short moment arm, the bending moment was not enough to cause roof to break. A wide shear plastic failure occurred to roof along the roadway strike, which conformed to the failure form of articulated point in the "S-R" instability theory of "masonry beam" [26]. The development of plastic zone in this roadway was mainly caused by mining disturbance in the upper section, so it was not included in analysis range of plastic zone in the stope with variable length. The roof near the open cut was undergoing shear failure, and the roof boundary on the upper side of goaf had undergone shear and tensile failure. Therefore, the two had a certain sequence in breaking time and space.

When 50 m was advanced, the range and value of shear stress on the upper side of the goaf gradually increased,

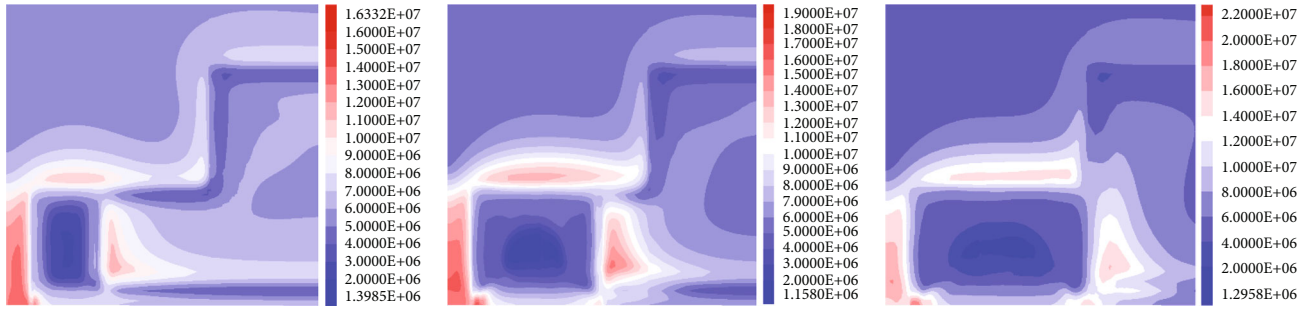

(a) Working face was advanced 25 m (b) Working face was advanced 50 m (c) Working face was advanced 75 m

Figure 24: Maximum shear stress of small mining stope.

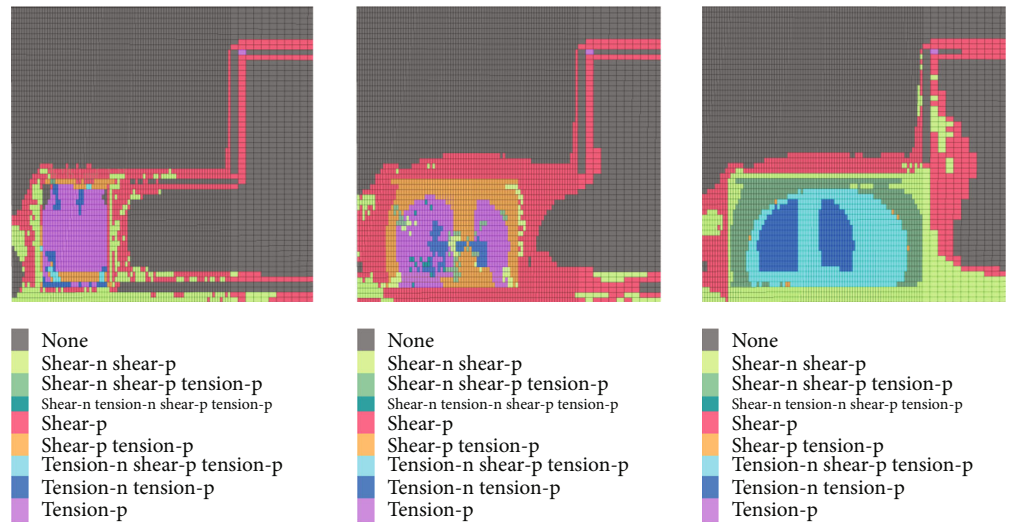

(a) Working face was advanced 25 m (b) Working face was advanced 50 m (c) Working face was advanced 75 m

Figure 25: Development of plastic zone in small mining stope.

and it was growing faster than the left and right sides. The main influence area of shear stress shifts to the long side of small mining stope. The roof above working face had a wide range of diffuse shear failure plastic zone and the goaf roof boundaries closed into an "O" shape, embedded shear and tensile failure plastic zone, the middle point exposed tensile failure plastic zone, in line with the "O-X" fracture in the roof center and the boundaries of their respective fracture characteristics. For the mechanical conditions of the lower boundary were very weak, the failure plastic zone in the middle was shifted downward.

When the working face was advanced 75 m, the shear stress range and bending moment of the goaf boundaries reached the maximum value, and the whole range of small mining stope roof was in dynamic activity stage of plastic failure. The "O-shaped" closure ring was dominated by dynamic shear failure, and the fracture in the center of the plate like an "X" shape was dominated by tensile failure; the shear and tensile mixed failure extended outwardly and blended with the plate boundaries, forming an "O-X" fracture.

To sum up, the upper boundary shear stress of small mining stope first reached the plate boundary breaking limit and shear failure occurred, and then, shear failure occurred at the left and right sides of the stope and formed "O-shaped" closure. Finally, the tensile failure occurred mainly in the center, and the shear and tensile failure extended outwards. When small mining stope was completely mined out, "O-X" plastic fracture will occur in the whole range. The broken law of the roof of small mining stope with three sides fixed and one side simply supported (the side simply supported is the long side) was verified.

3.3. Analysis of Mechanical Characteristics of Roof Fracture in Mutative Mining Stope. The first mining calculation of full-scale mining stope was the area of mutative mining stope. From the lengthening of the working face until the roof had obvious plastic zone, working face advance length was 40 m. The distribution characteristics of roof stress zone and plastic zone are shown in Figures 26 and 27.

In the lengthening stage of working face, the high stress concentration more than 25 MPa appeared at the right angle point of geological pillar. Shear stress range of roof near the working face ran through the whole length of working face, and the point stress concentration near roadway along goaf reached more than 25 MPa. The roof under such structural pressure will be prone to disaster.

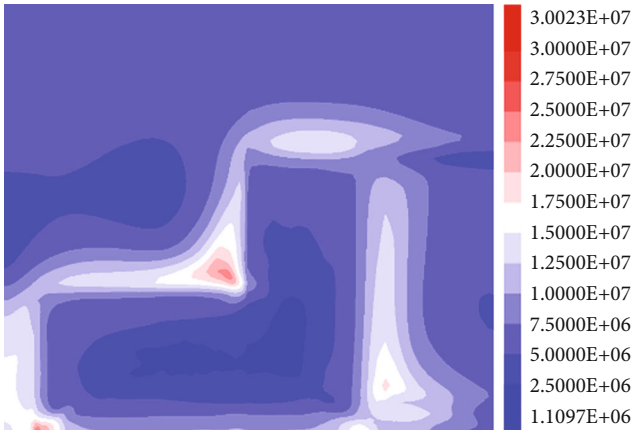

Figure 26: Maximum shear stress of mutative mining stope.

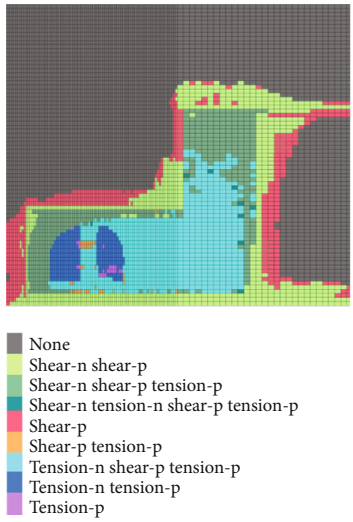

Figure 27: Development of plastic zone in mutative mining stope.

By comparison, the development degree of plastic zone of roof in mutative mining stope I and II was obviously different. Shear and tensile mixed plastic failure occurred in the whole roof of mutative mining stope I, which was the same as the failure form of goaf roof that adjacent small mining stope on the left. Moreover, both stopes have been surrounded by the "O" ring of the shear plastic zone, showing obvious continuity in the figure. Thus, the accuracy of the elongated "O-X" fracture was verified.

The plastic zone in the mutative mining stope II had a low degree of development, and shear and tensile mixed failure had occurred in the lower center position of roof and was connected with the plastic zone in mutative mining stope I. Considering that the depth of plastic zone along the strike of stope I was less than that along the inclined, it was sufficient to indicate that main development trend of plastic zone in mutative mining stope I was dip transfer to the II. Thus, the left "half-X-shaped" plastic fracture was formed, which verified the accuracy of the drift shape "O-X."

The shear failure had occurred at the right and left boundaries of mutative mining stope II, and tensile shear mixed failure had occurred at the lower part of the center. Therefore, the roof failure took lead in the above three positions. The upper boundary of this stope was undergoing shear failure, indicating that this was the last roof fracture boundary. The breaking sequence can be summarized as ① the left and right long sides break ⟶ ② the center of the plate breaks towards the lower part ⟶ ③ the upper short side breaks. It was the same as the breaking law of roof model with three sides fixed and one side simply supported (the simply supported side is the short side) mentioned above, which provided corresponding evidence for it.

3.4. Analysis of Mechanical Characteristics of Roof Fracture in Large Mining Stope. The last three mining calculations of full-scale mining stope were the area of the large mining stope, and the advancing length of the working face was 40 m, 40 m, and 30 m. The distribution characteristics of roof stress zone and plastic zone are shown in Figures 28 and 29.

The range and value of shear stress at the boundaries of large mining stope increased with the expansion of goaf. The right side and the upper side of the goaf were both fixed boundaries, and the shear force value on right side was generally 8-10 MPa higher than upper side. Therefore, the criterion about right boundary of roof breaks first was more sufficient.

When the working face of large mining stope advanced 40 m (the mining of full-scale mining stope was 80 m), the tensile and shear failure plastic zone expanded in a large range. The area where the roof in stope with variable length had previously undergone plastic failure and stability was transformed from static to dynamic, a new round of plastic failure evolution occurs, the elastic residual energy releases, and the roof of goaf sank further. In this process, roof near working face had been shear broken; the location of fracture was consistent with shear stress concentration area in stress diagram. This boundary was the first to fracture, shear and tensile failure plastic zone was interluded in the middle of newly advanced 40 m goaf roof, and shear failure was occurring at the upper boundary. The development characteristics of plastic zone were in accordance with roof fracture law of roof plate with both sides fixed and both sides simply supported (the simply supported sides are adjacent).

When the working face advanced 80 m (the full-scale mining stope was mined 120 m), shear and tensile mixed linear fracture zone along the strike appeared in middle of large mining stope, which reflected the continuous fracture characteristics of large mining stope roof to a certain extent. At this time, the roof cycle pressure step distance was short and the pressure was intense. The coal wall fracturing, roof caving, coal wall scaling, floor heaving, and other mining pressure showed the most serious, and the timeliness is extremely complex, which promoted the support pressure of large mining stope to increase continuously.

When the working face was advanced 110 m (the full-scale mining stope was mined 150 m), all the stope with variable length was completed, and boundaries were dominated by shear failure and interior was dominated by tensile failure. The fracture pattern of goaf roof tended to be stable,

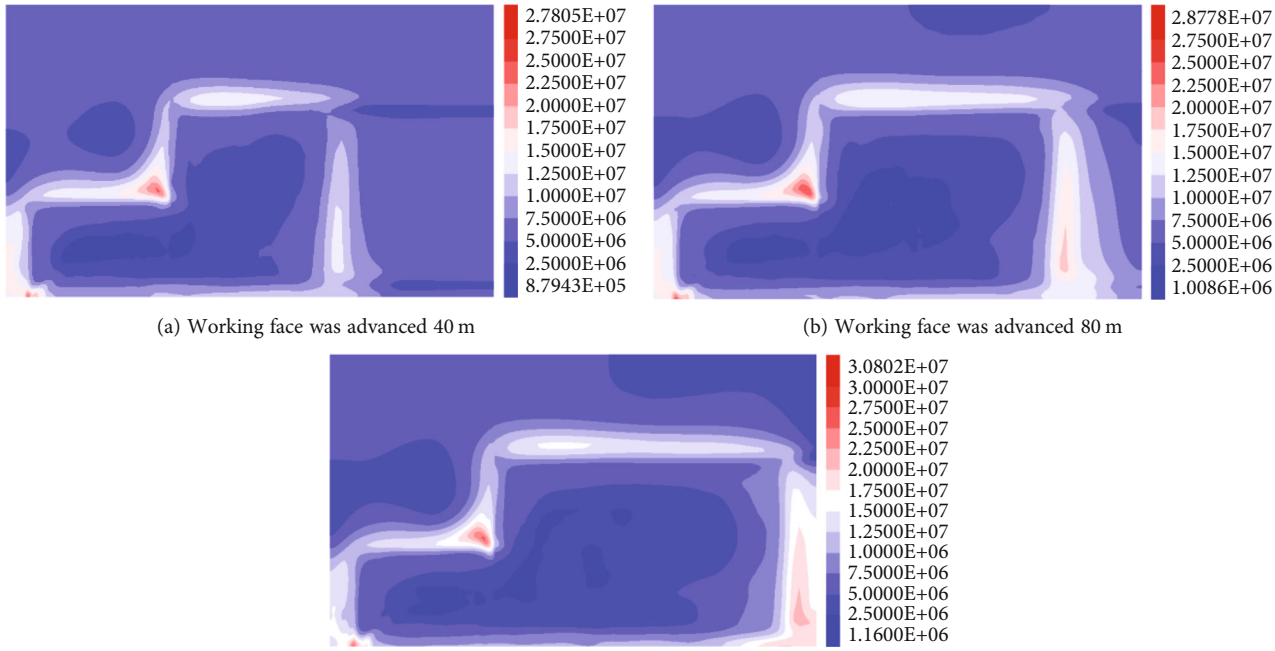

(a) Working face was advanced 40 m

(b) Working face was advanced 80 m

(c) Working face was advanced 110 m

Figure 28: Maximum shear stress of large mining stope.

but the vigorous activities of the roof will not stop, and dynamic subsidence was still taking place in the whole area.

3.5. Analysis of Mechanical Characteristics of Roof Fracture in Full-Scale Mining Stope. As shown in Figure 27, in mutative mining stope I, due to the continuous development of the plastic zone in small mining stope, the "half-X" shape of the shear and tensile fracture plastic zone was not obvious. However, an obvious "half-X" shape was formed in mutative face stope II, which could be identified as the developmental characteristics of plastic zone of the drift-shaped "O-X" fracture based on small mining stope or as the initial plastic zone development characteristics of the "X-O" fracture based on full-scale mining stope. Figure 29 shows the shear tensile fracture plastic zone. In (a), the development form of shear tensile plastic failure had occurred in new goaf, which spread from the middle to the right corner and formed a "half-X" shape on the other side. At this time, the "X" shape has been fully developed, and shear failure has occurred at the left, right, and upper boundaries of the mutative mining stope and large mining stope, forming the "X-C" fracture. Finally, the "C-shaped" plastic zone and roof of the roadway along the goaf form plastic circle closured, namely, the "X-O" fracture. In (b), the upper part of stope, a shear and tensile mixed linear fracture zone along the strike has appeared, that is, the central fracture extension zone of the prolongated "X-O" fracture.

It can be seen that the plastic zone development characteristics of FLAC^{3D} numerical analysis are very consistent with the fracture theory mentioned above, which provides a powerful engineering simulation basis for the fracture theory.

4. Mechanical Model and Structural Evolution Law of Roof Fracture in Stope with Variable Length

By summarizing the movement law of overlying strata, corresponding geometric structure and mining pressure characteristics of each stope mentioned above, the different mining pressure characteristics and fracture laws of the stope with variable length can be obtained compared with the normal stope. There are three different development stages of working face advancing from small mining stope to mutative mining stope to large mining stope. In small mining stope, the stoping space is small, the working face length is short, and it belongs to the stable pressure structure. The relatively regular "O-X" fracture occurs in roof, and mining pressure appears to ease, so it is called the stably static pressure mining area. When entering mutative mining stope, the length of working face changes abruptly, which belongs to the sudden pressure structure. The boundary conditions of roof become complicated, the continuity instability of rock structure will occur, and fracture tends to transfer. The prolongated "O-X" fracture and drift "O-X" fracture appear in the roof, the mining pressure transient time changes abnormally, and the mining space is broken and difficult to support, so it can be called the suddenly alterant pressure mining area. When it is advanced to large mining stope, the period of pressing step interval is short, and the roof fracture is regular. It belongs to increasing pressure structure, and the prolongated "X-O" fracture appears. The rock structure readjusted, the elastic residual energy is fully released, and the whole roof of stope with variable length is transformed from static stability to dynamic failure. The support resistance of mining space is high and has a trend

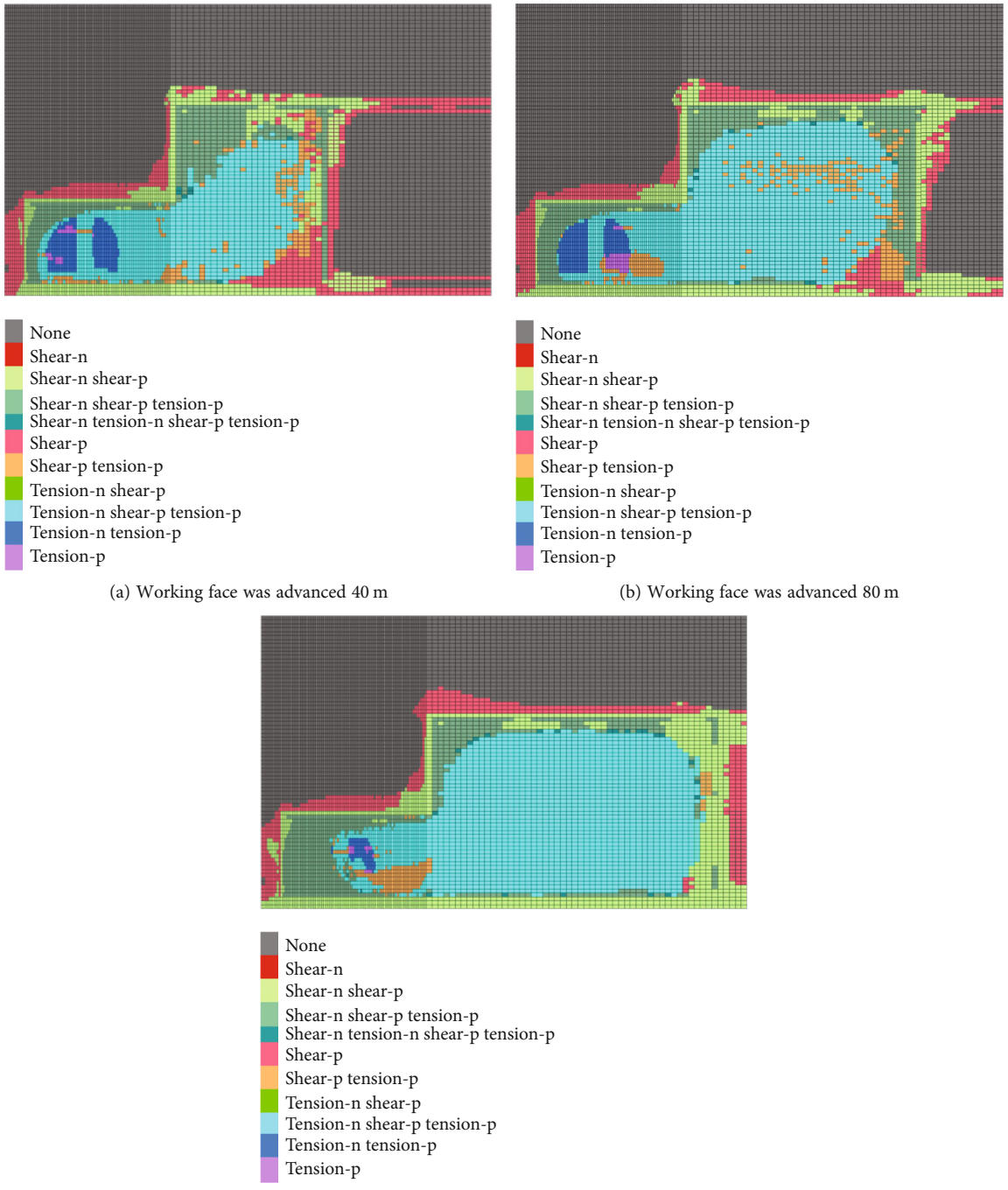

(a) Working face was advanced 40 m

(b) Working face was advanced 80 m

(c) Working face was advanced 110 m

Figure 29: Development of plastic zone in large mining stope.

of continuous growth, so it is called the increasingly dynamic mining area. The overburden structure pressure model of "three stopes, three areas, and three structures" is derived, as shown in Figure 30.

Mutative mining stope and large mining stope are integrated into full-scale mining stope, and the complex "half-X-shaped" fracture was developed from the irregular fracture in the center of mutative mining stope I and II. The fracture was combined with the central fracture of large mining stope to form an "X-shaped" fracture, and then, the peripheral fracture of full-scale mining stope was connected to form a "C-shaped" fracture, finally closed into the "X-O" form of breaking law. This is contrary to the traditional "O-X" form of fracture law in small mining stope, but it will occur with the advance of working face prolongated fracture. Thus, the roof breaking theory of "two stopes and two laws" in stope with variable length is derived, as shown in Figure 31.

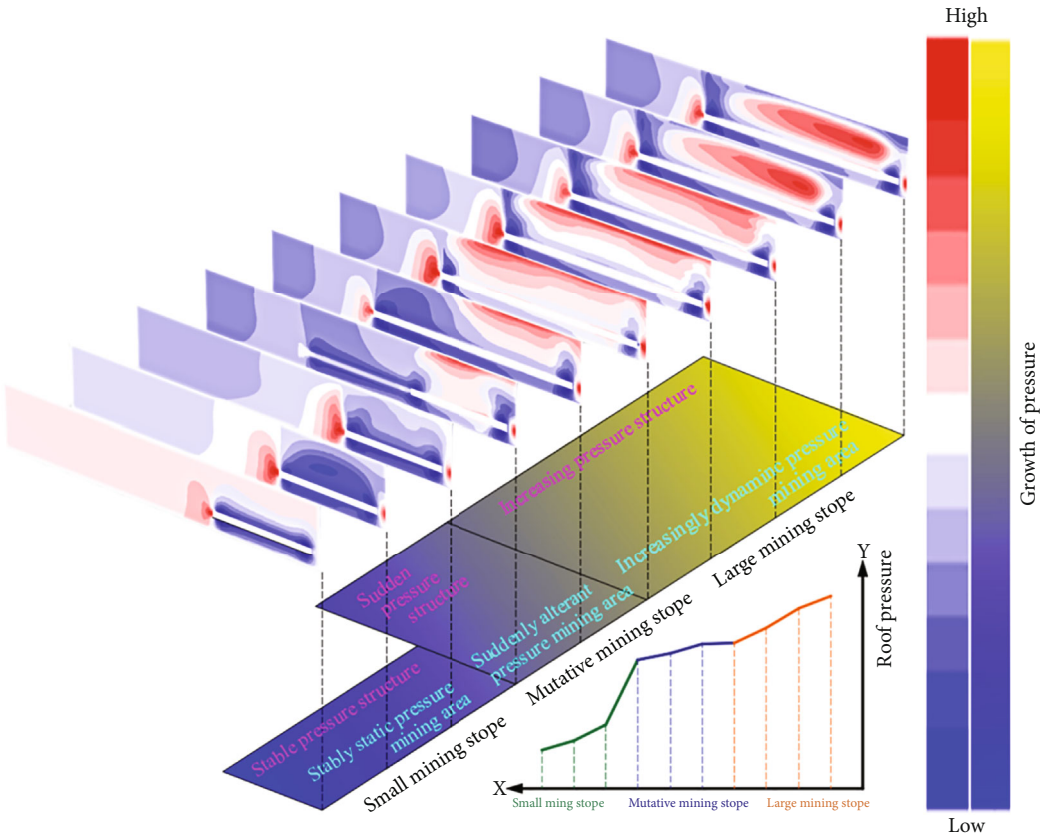

Figure 30: Pressure model of overburden structure of "three stopes, three areas, and three structures."

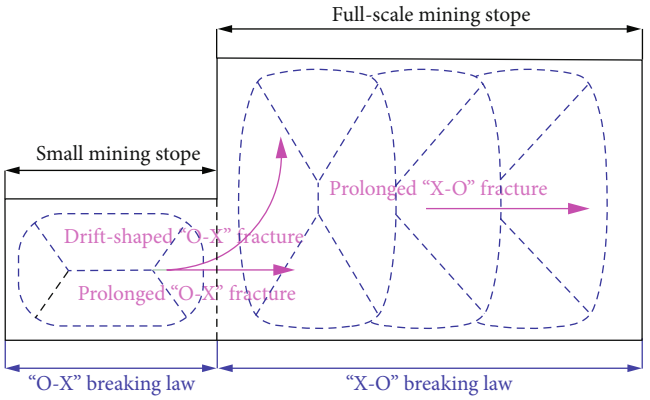

Figure 31: "Two stopes and two laws" roof fracture theoretical model.

It should be pointed out that, if the working face advances from full-scale mining stope to small mining stope, the overburden structural pressure and fracture law are also different, because of the different boundary conditions, so this theory is only applicable to process of advancing from small mining stope to full-scale mining stope at present.

5. Conclusions

(1) According to actual geological characteristics and working face layout characteristics of the stope with variable length, the theory of thin plate bending with small deflection of elasticity was applied to establish roof elastic model with three sides fixed and one simply supported (the simply supported side is the long side), one side fixed and three sides simply supported, one simply supported with three sides fixed (the simply supported side is the short side), and both sides fixed and both simply supported (the simply supported sides are adjacent). Through the roof breaking law of mathematical solution, the "O-X" fracture process of small mining stope, prolongated "O-X" fracture process, and drifting "O-X" fracture process of mutative mining stope, as well as the "X-O" fracture process and prolongated "X-O" fracture process of full-scale mining stope were deduced

(2) Using FLAC^{3D} to carry out engineering simulation, the evolution process of stress zone and plastic zone was obtained, which fully conformed to the calculation results of mathematical mechanics model. It provided a strong support for the breaking law of the stope with variable length, especially for the breaking law of the full-scale mining stope

(3) The roof "O-X" fracture rule of small mining stope is as follows: ① the long fixed side fracture on the upper part ⟶ ② the short fixed side fracture on both sides extending ⟶ ③ the "O-shaped" closure with the broken roof along the goaf ⟶ ④ the

central fracture ⟶ ⑤ "X-shaped" penetration → ⑥ "O-X" fracture law is formed. The roof "X-O" fracture law of the full-scale mining stope is as follows: ① left short simple and fixed side fracture ⟶ ② "half-X-shaped" fracture ⟶ ③ long fixed side and plate center fracture extension promote short fixed side fracture ⟶ ④ "X-C-shaped" fracture ⟶ ⑤ "O-shaped" closure formed by the broken roadway along the goaf ⟶ ⑥ "X-O" fracture law formed

(4) The causes and accompanying phenomena of mining pressure in small mining stope, mutative mining stope, and large mining stope were summarized, and the "three stopes, three areas, and three structures" overburden structure pressure model for stope with variable length was put forward. The roof fracture forms of small face stope and large face stope were summarized, and the theoretical model of "two stopes and two laws" roof fracture of stope with variable length was put forward (only applicable to the process of working face from short to long)

Data Availability

The data used to support the findings of this study are included within the article.

Conflicts of Interest

The authors declare that they have no conflicts of interest regarding the publication of this paper.

Acknowledgments

This work is supported by the National Natural Science Foundation of China (Grant No. 51904266), excellent youth project of Hunan Provincial Department of Education (Grant No. 21B0144), and Research Project on Teaching Reform of Colleges and Universities in Hunan Province in 2020 (Grant No. HNJG-2020-0231).

References

[1] M. C. He, H. P. Xie, S. P. Peng, and Y. D. Jiang, "Study on rock mechanics in deep mining engineering," *Chinese Journal of Rock Mechanics and Engineering*, vol. 24, no. 16, pp. 2803–2813, 2005.

[2] L. U. Bang-Wen, L. I. Chang-Wu, X. I. Hui, H. E. Tao, and W. A. Ding, "Law of overburden strata movement and mining roadway deformation under mining influence in the unequal length of working face," *Metal Mine*, vol. 45, no. 1, pp. 34–38, 2016.

[3] L. Yang-yang, Z. Shi-chuan, G. Li-qun, K. De-zhi, and K. He, "Mechanism and prevention of pressure burst in step region based on overburden strata movement of unequal length working face," *Rock and Soil Mechanics*, vol. 37, no. 11, pp. 3283–3290, 2016.

[4] X. F. Wang, *Slope Length Effect of Roof Fracture Mechanism and Stress Distribution Characteristics of Irregular Stope*, AnHui University of Science and Technology, Huainan, 2015.

[5] J. G. Ning, J. Wang, Y. L. Tan, and Q. Xu, "Mechanical mechanism of overlying strata breaking and development of fractured zone during close-distance coal seam group mining," *International Journal of Mining Science and Technology*, vol. 30, no. 2, pp. 207–215, 2020.

[6] Y. Y. Liu, X. M. Song, and D. F. Zhu, "Dynamic structural mechanical behavior and response characteristics of large key blocks," *Rock and Soil Mechanics*, vol. 41, no. 3, pp. 1019–1028, 2020.

[7] F. Cui, C. Jia, X. P. Lai, and J. Q. Chen, "Study on the evolution characteristics and stability of overburden structure in upward mining of short distance coal seams with strong burst tendency," *Chinese Journal of Rock Mechanics and Engineering*, vol. 39, no. 3, pp. 507–521, 2020.

[8] F. X. Jiang, "Viewpoint of spatial structures of overlying strata and its application in coal mine," *Journal of Mining and Safety Engineering*, vol. 23, no. 1, pp. 30–33, 2006.

[9] Y. Xue, T. Teng, and X. H. Wang, "Analysis of fracturing model and caving law of stope roof," *Science Technology and Engineering*, vol. 16, no. 7, pp. 156–161, 2016.

[10] H. Yu, *Study on the Movement of Upper Strata and the Pressure Behavior Law of Close Distance Coal Seams*, China University of Mining & Technology, Beijing, Beijing, 2015.

[11] W. A. Xin-Feng, G. A. Ming-Zhong, C. H. Yu-Xue, W. A. Jian-Jian, L. A. Xue-Qiang, and Z. H. An-Wei, "Analysis of fracturing characteristics of stope roof based on elastic thin plate theory," *Metals and Minerals*, vol. 50, no. 6, pp. 24–28, 2015.

[12] H. Wang, Z. Chen, Z. Du, and J. Li, "Application of elastic thin plate theory to change rule of roof in underground stope," *Chinese Journal of Rock Mechanics and Engineering*, vol. 25, no. S2, pp. 3769–3774, 2006.

[13] F. He, H. Wenrui, D. Chen, S. Xie, H. Li, and C. He, "First fracture structure characteristics of main roof plate considering elastic-plastic deformation of coal," *Journal of China Coal Society*, vol. 45, no. 8, pp. 2704–2717, 2020.

[14] D. D. Chen, S. R. Xie, and F. L. He, "Fracture rule of main roof thin plate with the elastic foundation boundary and long side coal pillar," *Journal of Mining & Safety Engineering*, vol. 35, no. 6, pp. 1191–1199, 2018.

[15] D. D. Chen, F. L. He, and S. R. Xie, "Time-space relationship between periodic fracture of plate structure of main roof and rebound in whole region with elastic foundation boundary," *Chinese Journal of Rock Mechanics and Engineering*, vol. 35, no. 6, pp. 1191–1199, 2018.

[16] Y. G. Wang, W. B. Guo, E. H. Bai et al., "Characteristics and mechanism of overlying strata movement due to high-intensity mining," *Journal of China Coal Society*, vol. 43, no. S1, pp. 28–35, 2018.

[17] W. A. Hong-sheng, L. I. Shu-gang, Z. H. Xin-zhi, W. U. Lin-zi, D. O. Yong-jian, and S. H. Hai-qing, "Analysis on stability of narrow coal pillar influenced by main roof fracture structure of gob-side roadway," *Coal Science and Technology*, vol. 42, no. 2, pp. 19–22, 2014.

[18] X. F. Wang, M. Y. Lu, Y. H. Gao, W. B. Luo, and W. G. Liu, "Structural mechanical characteristics and instability law of roof key block breaking in gob-side roadway," *Advances in Civil Engineering*, vol. 2020, Article ID 6682303, pp. 1–12, 2020.

[19] G. R. Feng and P. F. Wang, "Stress environment of entry driven along gob-side through numerical simulation

incorporateing the angle of break," *International Journal of Mining Science and Technology*, vol. 30, pp. 189–196, 2020.

[20] C. J. Hou, X. Y. Wang, J. B. Bai, N. K. Meng, and W. D. Wu, "Basic theory and technology study of stability control for surrounding rock in deep roadway," *Journal of China University of Mining and Technology*, vol. 50, no. 1, pp. 1–12, 2021.

[21] H. Wu, B. Dai, L. Cheng, R. Lu, G. Zhao, and W. Liang, "Experimental study of dynamic mechanical response and energy dissipation of rock having a circular opening under impact loading," *Mining, Metallurgy & Exploration*, vol. 38, no. 2, pp. 1111–1124, 2021.

[22] R. Cheng, Z. Zhou, W. Chen, and H. Hao, "Effects of axial air deck on blast-induced ground vibration," *Rock Mechanics and Rock Engineering*, vol. 55, no. 2, pp. 1037–1053, 2021.

[23] R. Cheng, W. Chen, and H. Hao, "A state-of-the-art review of road tunnel subjected to blast loads," *Tunnelling and Underground Space Technology*, vol. 112, p. 103911, 2021.

[24] F. Feng, S. J. Chen, Y. J. Wang, W. P. Huang, and Z. Y. Han, "Cracking mechanism and strength criteria evaluation of granite affected by intermediate principal stresses subjected to unloading stress state," *International Journal of Rock Mechanics and Mining Sciences*, vol. 143, p. 104783, 2021.

[25] Z. L. Xu, *Easticity*, Higher Education Press, Beijing, 2015.

[26] M. G. Qian, P. W. Shi, and J. L. Xu, *Mining Pressure and Strata Control*, China University of Mining and Technology Press, Xuzhou, 2010.